BELLCOMM, INC.
1100 SEVENTEENTH STREET, N.W. WASHINGTON, D.C. 20036

COVER SHEET FOR TECHNICAL MEMORANDUM

TITLE- S-IVB Attitude During Transposition, Docking and Withdrawal on Lunar Missions

TM- 68-2013-1

DATE- May 15, 1968

FILING CASE NO(S)- 310

AUTHOR(S)- L. P. Gieseler

FILING SUBJECT(S)- (ASSIGNED BY AUTHOR(S)- Transposition, Docking, Attitude Maneuver, Lighting, Withdrawal, Communications

(NASA-CR-95433) S-4B ATTITUDE DURING TRANSPOSITION, DOCKING AND WITHDRAWAL ON LUNAR MISSIONS (Bellcomm, Inc.) 40 p
N79-72321
Unclas
00/18 11172
FF No.
(NASA CR OR TMX OR AD NUMBER) (CATEGORY)
[redacted]

ABSTRACT

In many cases the lighting conditions at transposition, docking, and withdrawal can be considerably improved by rotating the S-IVB about the antenna axis to a preferred position. Giving the S-IVB communication constraint first priority, the LM withdrawal illumination constraint will not be satisfied for lunar landing sites east of about 3° west longitude in the worst case, and will not be satisfied for sites east of about 7° east longitude in the best case. The best case corresponds to translunar trajectories having high inclinations relative to the lunar orbit plane.

Hardware modifications involving the use of springs for separating the S-IVB from the spacecraft and for ejecting the SLA panels are under consideration. These modifications, if made, will allow relaxation of the withdrawal illumination constraint.

The relationships between lighting and communication conditions in view of present constraints during the transposition, docking, and withdrawal maneuver of the Apollo mission are analyzed using a simplified physical model. Five constraints are considered: (1) Satisfactory communication between the earth and the S-IVB during the transposition and docking maneuver, (2) Satisfactory illumination of the S-IVB and SLA by the sun during withdrawal, (3) A limit on the magnitude of the S-IVB allowable yaw maneuver, (4) A restriction on the angle between the -x axis of the CSM and the sun during docking, and (5) A restriction on the elevation of the sun at lunar landing to the range between 7 and 20 degrees above the eastern horizon. These constraints are collectively considered analytically to determine the allowable S-IVB attitudes.

SEE REVERSE SIDE FOR DISTRIBUTION LIST

DISTRIBUTION

COMPLETE MEMORANDUM TO

CORRESPONDENCE FILES:

OFFICIAL FILE COPY
plus one white copy for each
additional case referenced

TECHNICAL LIBRARY (4)

NASA Headquarters

Mr. T. A. Keegan/MA

MSC

Messrs. J. R. Gurley/FM13
M. V. Jenkins/FM
M. D. Jenness/FM5
J. A. McAnulty/FM13
R. J. Ward/PD12

MSFC

Messrs. R. E. Beaman/I-V-E
J. W. Cremin/R-AERO-DAP
E. T. Deaton/R-AERO-DA
O. M. Hardage/R-AERO-FM
G. Wittenstein/R-AERO-FMT

Bellcomm

Messrs. D. R. Anselmo
A. P. Boysen, Jr.
J. O. Cappellari, Jr.
D. A. Corey
D. A. DeGraaf
D. R. Hagner
W. G. Heffron
J. J. Hibbert
B. T. Howard
D. B. James
S. L. Levie, Jr.
J. L. Marshall, Jr.

Bellcomm (contd.)

Messrs. J. Z. Menard
V. S. Mummert
B. G. Niedfeldt
P. E. Reynolds
F. N. Schmidt
R. V. Sperry
J. W. Timko
R. L. Wagner
All Members, Department 2013
Department 1023

Cover Sheet Only To

Messrs. D. A. Chisholm
I. M. Ross

BELLCOMM, INC.
1100 Seventeenth Street, N.W. Washington, D.C. 20036

SUBJECT: S-IVB Attitude During Transposition, Docking, and Withdrawal on Lunar Missions - Case 310

DATE: May 15, 1968

FROM: L. P. Gieseler

TM-68-2013-1

TECHNICAL MEMORANDUM

1.0 INTRODUCTION

This memorandum is concerned with the selection of the best inertial attitude of the S-IVB during transposition, docking, and withdrawal and the maneuver required to attain this attitude. A simplified sun-earth-moon system is used, making possible an analytical formulation of the problem. The emphasis is on gaining insight rather than solving the problem for a particular launch date.

The body of the memorandum presents the relevant constraints (Section 2.0); the characteristics of a typical translunar trajectory in a reference lunar-orbit-plane coordinate system (Section 3.0); S-IVB vehicle attitude considerations in light of the communications constraint during transposition, docking and withdrawal (Section 4.0); the expected position of the sun in the reference coordinate system for the range of lunar landing sites under consideration (Section 5.0); the incident illumination on the LM and SLA during docking and withdrawal (Section 6.0); the maneuvers required to reach the best attitude (Section 7.0); hardware modifications (Section 8.0); and finally the conclusions (Section 9.0). Appendix I gives a list of symbols and their definitions. Derivation of the equations governing attitude and attitude maneuvers in the three-dimensional case are considered in Appendices II and III. A method for computing the gimbal angles of the S-IVB stable platform is given in Appendix IV.

2.0 CONSTRAINTS

During the first three hours after translunar injection (TLI) the range from the vehicle to the earth increases from about 150 n.mi. to nearly 30,000 n.mi. and the angle subtended by the earth, as viewed from the S-IVB, decreases from about 146° to approximately 14°. The earth-vehicle line rotates through an angle of 125°. The S-IVB will be maintained at a constant inertial attitude during the transposition, docking and withdrawal maneuvers, which nominally will occur between TLI plus .25 hours and TLI plus 2 hours. Hence, the position of the earth as seen from the S-IVB will change considerably during these maneuvers. The position of the sun, however, will remain nearly constant.

Five constraints are especially important during this portion of an Apollo lunar mission:

1. Communication is required during the transposition and docking period between the S-IVB and the earth. (Reference 1, Section 1.0). The approximate direction of the antenna axis is shown in Figure 1.

2. A line drawn from the S-IVB to the sun should pass through the shaded area shown in Figure 1, to insure satisfactory illumination during the withdrawal of the LM from the S-IVB. (Reference 1, Section 4.0).

3. Attitude maneuvers should be such that the angle between the S-IVB x axis and the earth parking orbit plane should not exceed 45°. This constraint is a result of a limitation on the Saturn stable platform middle gimbal angle. (Reference 1, Section 1.1.3).

4. The angle between the x axis of the CSM and the sun should not be greater than 90° during docking. This will prevent glare on the S-IVB/LM from interfering with visibility from the CSM.

5. The elevation of the sun above the eastern horizon at the lunar landing site should lie between 7 and 20 degrees.

3.0 TRAJECTORY CONSIDERATIONS

Figures 2 and 3 show the simplified sun-earth-moon system used. The x axis has a fixed inertial direction, and is taken to be the earth-moon line when the spacecraft is at periselene. The xy plane coincides with the lunar orbital plane with the y axis directed as shown in Figure 3. The vector $\overline{R}_{sun}$, which points to the sun, is also located in the xy plane and makes an angle θ_{sun} with the -y axis. The elevation of the sun above the eastern horizon of the lunar landing site is equal to the angle between $\overline{R}_{sun}$ and the local horizon. This angle determines the lighting conditions at lunar landing.

The characteristics of a typical translunar ellipse were taken from Reference (2), the quantities used are:

$\bar{R}_1$ radius vector at translunar injection (TLI) ($|\bar{R}_1| = 2.206 \times 10^7$ ft.)

V velocity at TLI (35,500 ft/sec)

β flight path angle at TLI (7.6°)

θ_1 angle between $\bar{R}_1$ and the +x axis (156°)

The first three quantities are sufficient to define the shape of the ellipse. The angle between the semi-major axis and the x axis (θ_A) can be determined with sufficient accuracy by Equation (1).

$$\theta_A = 180 - \theta_1 - 2\beta \tag{1}$$

The simplifying assumption is made that the true anomaly is twice the flight path angle.

The vector $\bar{R}_S$ is directed from the center of the earth to any point on the ellipse. The corresponding angle θ_S, as shown in Figure 3, can be calculated from Equation (2) below, with θ_A and the true anomaly, f_S, specified.

$$\theta_S = 180 - \theta_A - f_S \tag{2}$$

The need for the angle θ_S will become clear in Section 6 where the lighting constraint at withdrawal is discussed.

4.0 VEHICLE ATTITUDE CONSIDERATIONS

The S-IVB body coordinate system is designated by the unit orthogonal vectors XV, YV, and ZV which are also the axes of rotation for roll, pitch, and yaw respectively. Between TLI + 0 and TLI + 1 min. the vehicle is held at a fixed inertial attitude. Between TLI + 1 min. and TLI + 15 min. the vehicle is oriented with XV along the local horizontal and ZV toward the center of the earth. YV is directed into the xy plane of Figures 2 and 3. The vehicle is then maneuvered to an attitude which will remain fixed during the transposition and docking period. This attitude is selected to satisfy, if possible, the first four constraints listed in Section 2. The fifth constraint, lighting at lunar landing, is satisfied by proper selection of the launch date. The communication constraint (No. 1) is considered to be more important than the lighting constraints (Nos. 2 and 4).

For the analysis which follows, the assumption is made that the antennas of the S-IVB are pointed exactly in the +ZV direction and that the antenna pattern has a circular symmetry about the +ZV axis.

A reference orientation is established in which the +ZV axis points to the center of the earth at TLI + 2 hours and both ZV and XV axes lie in the vehicle orbital plane. From Figure 2 it can be seen that the ZV axis will point to the left of the center of the earth before TLI + 2 hours, and to the right of it after TLI + 2 hours. This is demonstrated in Figure 4, where the angle between the ZV axis and the earth-vehicle line is plotted against range to the surface of the earth. This angle equals 55° at TLI + .25 hours when set to zero at TLI + 2 hours, and will reach -7° at TLI + 3 hours. The angular relationship for the line from the vehicle to the east and west limbs of the earth is also shown. (For the same vehicle position the range for these two cases is larger by approximately the radius of the earth.)

The dotted curves of Figure 4 show approximately the limit of satisfactory communication between the earth and the S-IVB for various off-axis angles. It can be seen that from TLI + 1 hour to TLI + 3 hours the entire earth is within the communication boundaries. For times less than one hour there will be difficulty communicating with stations east of the earth's sub-vehicle point. This condition could be alleviated somewhat if the vehicle were oriented so that the ZV axis pointed about 10° to the east of the center of the earth, or by using TLI + 1.5 hours for the reference attitude. This orientation would, however, limit communication near the west limb at the 3-hour point.

5.0 LIGHTING CONDITIONS AT LUNAR LANDING

As shown in Figure 3 the moon moves from A to B during the time that the spacecraft is in the lunar parking orbit. It also rotates through an angle θ_B. The value of θ_B used in this memorandum was determined from the following assumptions:

1. Number of lunar parking orbit revolutions prior to landing = 10.

2. Time per revolution in parking orbit = 2 hours.

3. Angular velocity of the moon = .5°/hr.

Then $\theta_B = 10 \times 2 \times .5 = 10°$. The elevation of the sun above the eastern horizon for a lunar landing site having a longitude (λ_s) of zero equals $\theta_{sun} + \theta_B$. The elevation of the sun (E_{sm}) at any longitude may be determined by evaluating the following relationship:

$$E_{sm} = \theta_{sun} + \theta_B + \lambda_s \tag{3}$$

The angles λ_s and E_{sm} are restricted to the range $-45° < \lambda_s < +45°$ and $7° < E_{sm} < 20°$ respectively. In this simplified model the sun is assumed to remain fixed during the time interval between the transposition and docking maneuver and lunar landing (about 3 days). This will introduce an error of about 3° in the sun direction at transposition and docking.

6.0 LIGHTING CONDITIONS DURING TRANSPOSITION, DOCKING, AND WITHDRAWAL

The important parameter for determining lighting conditions during transposition, docking, and withdrawal is $\Delta\theta$, the angle between $\overline{R}_{sun}$ and the XV axis. As mentioned previously, in the reference orientation the ZV axis is aligned along the $-\overline{R}_{S2}$ direction, where $\overline{R}_{S2}$ is the position vector of the point on the ellipse at TLI + 2 hours. The ZV and the XV axes lie in the vehicle orbital plane. For the case where the translunar trajectory is in the earth-moon plane, they also lie in the xy plane. Then from inspection of Figure 3,

$$\Delta\theta = |\theta_{S2} - \theta_{sun}| \tag{4}$$

For out-of-plane cases $\overline{R}_{sun}$ is assumed to remain in the XY plane, but the vehicle orbital plane is rotated about the x axis through the angle DL, the dihedral angle between the vehicle and the lunar orbital planes. During the 1969-1970 period this angle varies from 0 to 62 degrees depending somewhat on the launch azimuth but mainly on the lunar declination. The relationship between DL and the lunar position for the two injection types (Atlantic and Pacific) is shown in Figure 5. The relationship between the angular position of the moon and date is given in Table I for 1969. By rotating the vehicle orbital plane as described above, the trajectory of Reference (2) can be used to consider all practical ranges of launch azimuth and launch date. Additional information about the angle DL, including the formulas that determine Figure 5, is given in Reference (3), Appendix II.

The angle $\Delta\theta$ is computed from the formula:

$$\Delta\theta = \cos^{-1} (\bar{X}V \cdot \bar{R}_{sun}) \qquad (5)$$

The computation of $\bar{X}V$ as a function of $\bar{R}_{S2}$ and DL is discussed in Appendix II. Figure 6 is a plot of $\Delta\theta$ against λ_S for various values of DL, and for the reference orientation. E_{sm} was assumed to equal 10°. When DL = 0 Equation (4) is valid. Since θ_{S2} is constant it can be seen from the equation that the relationship is a straight line having a slope of $\pm$ 1. The lighting constraint for the maneuver is given by the inequality $|\Delta\theta| < 34°$, as indicated in the figure. When DL = 0 this constraint is exceeded for values of λ_S greater than -3°. As one would expect, $|\Delta\theta|$ becomes larger as DL increases from 0° to 60° and the lighting conditions become worse.

6.1 Rotation of the Vehicle About the ZV Axis

In Figure 7 the vehicle has been rotated about the ZV axis (the yaw axis) until $|\Delta\theta|$ is minimized. (Constraints on the maximum allowable Saturn yaw are ignored for the present.) The details of the calculation of $\overline{XV}$ for this case are also given in Appendix II. A yaw maneuver cannot reduce $\Delta\theta$ in the case where DL = 0, and therefore the relationship between $\Delta\theta$ and λ_S is the same as that shown in Figure 6. This is clear from Equation (8) of Appendix II which shows that the value of $\overline{XV}$ producing minimum $|\Delta\theta|$ must lie in the R_{sun}, R_{S2} plane; however, $\overline{XV}$ is in that plane for DL = 0.

A marked improvement in the minimum value of $|\Delta\theta|$ is possible when DL $\neq$ 0. When DL = 60° (approximately the maximum it can attain), λ_S can now be increased from -3° to +22° before the illumination constraint is violated. For the case DL = 60° and λ_S = 0, $\Delta\theta$ is reduced from 67° to 18° by yawing the vehicle.

6.2 S-IVB Yaw Constraint

The middle gimbal angle measures the amount that the S-IVB x axis has been rotated out of the plane of the earth parking orbit. The value of the angle (θ_m) was calculated using the equations of Appendix IV. Many values of DL and λ_S lead to values of $|\theta_m|$ greater than 45°. Figure 8 shows the relationship between $\Delta\theta$, λ_S and DL when the constraint $|\theta_m| < 45°$ is added. Details of the calculation of $\overline{XV}$ are given in Appendix II, and a description of the gimbal system is given in Appendix IV. From Figure 8 it can be seen that when DL = 60°, λ_S can be increased to +7° before the lighting constraint is violated. Comparing the data on Figures 7 and 8 for the case DL = 60° and λ_S = 0, $\Delta\theta$ equals 29° instead of the 18° obtained without the restriction $|\theta_m| < 45°$.

6.3 Additional Considerations

A further restriction imposed by the lighting conditions during withdrawal involves the projection of $\overline{R}_{sun}$ on the YV-ZV plane. As shown in Figure 1 the angle $\Delta\theta_1$ which this vector makes with the -YV axis should not be smaller than 30°. It is shown in Appendix II that this projection of $\overline{R}_{sun}$ always coincides with the ZV axis if the vehicle is rotated about $\overline{ZV}$ until $|\Delta\theta|$ is minimized. $\Delta\theta_1$ then always equals 90°, regardless of the value of DL and θ_{sun}, and the restriction is not violated for the cases plotted in Figure 7.

When the constraint $|\theta_m| < 45°$ is added, $\Delta\theta_1$ may assume values different from 90°. However in most of the cases represented by Figure 8, $\Delta\theta_1$ was greater than 30°. The quantities $\Delta\theta$ and λ_S are independent of the sign of DL, and therefore only positive values are plotted in Figures 6, 7, and 8. However, $\Delta\theta_1$ does depend upon the sign of DL, and as indicated in Figure 8, the constraint on $\Delta\theta_1$ is violated only when DL approaches +60°. This situation occurs rather infrequently; a check of launch opportunities in 1969 reveals that 2 out of 48 trajectories have values of DL greater than 55 degrees. Note that $\Delta\theta$ for these cases is less than 15°, and therefore $\overline{R}_{sun}$ goes through the excluded area of Figure 1 near the apex of the wedge.

An additional constraint (No. 4 of Section 2.0) requires that the angle between the -x axis of the active vehicle and the sun be not greater than 90° during docking. (Reference 1, paragraph 4.1.2) The active vehicle is the CSM, whose -x axis points in the same direction as the +x axis of the S-IVB during docking. The angle involved is $\Delta\theta$, the same angle plotted in Figure 8. It can be seen that $\Delta\theta$ is less than 90° for the worst case (DL = 0); therefore, this constraint is always satisfied.

Equation (3) can be used to extend the results of Figures 6, 7, and 8 to values of E_{SM} other than 10°. The number of lunar parking revolutions prior to landing can also be different from 10. The necessary adjustments to the figures are given below:

For E_{sm} = 7°, shift the λ_S scale 3° to the right

For E_{sm} = 20°, shift the λ_S scale 10° to the left

For 9 LPO revolutions shift the λ_S scale 1° to the left

For 11 LPO revolutions shift the λ_S scale 1° to the right

7.0 ATTITUDE MANEUVERS

The S-IVB must be changed from the local horizontal attitude shown in Figure 3 at TLI + .25 hours to the attitude shown at TLI + 2 hours. Two maneuvers for the in-plane case (DL=0) can be determined from inspection of the figure. Assume for simplicity that the ZV1 and the y axis are parallel. Note that the YV axis at TLI + .25 hours is directed into the plane of the paper, whereas at TLI + 2 hours it is directed out of the paper. From the figure it can be seen that a rotation of 180° about the XV axis (roll) followed by a negative rotation about the new YV axis (pitch) by $90° + \theta_{S2}$ will perform the required conversion. A rotation of $(90 + \theta_{S2})$ about the YV axis followed by a rotation of 180° about the new XV axis will also work. In addition, a single rotation of 180° about a line which bisects the angle between $\overline{XV1}$ and $\overline{XV2}$ will perform the required attitude change. This line is indicated by A-A in Figure 3. The angle between A-A and the x axis is one-half the angle that $\overline{XV2}$ makes with the x axis and equals $45° + \theta_{S2}/2$ as shown in the figure.

For the case where the translunar trajectory is not in the lunar orbital plane ($DL \neq 0$), three successive rotations are generally required. The theory of these rotations and a method of calculating the required angle is explained in Appendix III. As indicated there it is also possible in this case to perform an attitude change by means of a single rotation. The axis of rotation is not generally aligned with the vehicle coordinate axes.

8.0 HARDWARE MODIFICATIONS AFFECTING WITHDRAWAL ILLUMINATION CONSTRAINTS

Two modifications to existing hardware are being considered which will affect the withdrawal lighting constraint (constraint 2 of Section 2.0). A system of springs may be used rather than the SM RCS for separation of the CSM/LM combination from the S-IVB. The SLA panels may be ejected rather than swinging open as is done at present. The extent of the relaxation of the constraint will depend upon simulations yet to be performed. The docking constraint (constraint 4 of Section 2.0) would probably be unaffected by these changes. However as indicated in Section 6.0 the withdrawal constraint is the one that is violated for eastern lunar landing sites. A relaxation of the withdrawal illumination constraint to the docking constraint would allow all constraints to be met for lunar landing sites in the longitude range of $\pm 45°$.

9.0 CONCLUSIONS

Satisfactory communication between the S-IVB and the earth from TLI + 1 hour to TLI + 2 hours is achieved by orienting the S-IVB so that its antennas point to the center of the earth at TLI + 2 hours. At times earlier than TLI + 1 hour there may be difficulty communicating with ground stations located east of the sub-vehicle point on the earth. This can be alleviated somewhat by changing the orientation of the S-IVB so that the antennas point about 10° to the east of the center of the earth at the TLI + 2 hour point. For this attitude the communication at TLI + 2 hours still appears to be satisfactory.

The angle between the earth-moon line and a vector pointing to the sun can change as much as 103° as the lunar landing site longitude is varied from -45° to +45° and the elevation of the sun at the lunar landing site is varied from 7° to 20°. A similar variation in angle between the S-IVB x axis and the sun vector at transposition, docking, and withdrawal will occur unless the attitude of the S-IVB is properly adjusted for each mission opportunity.

For in-plane trajectories (DL = 0) the communication constraint prevents any adjustment of S-IVB attitude except for a variation of about 10° made possible by the width of the antenna pattern. It is shown that for lunar landing longitudes east of 3° west longitude the lighting conditions during the withdrawal maneuver are outside the present limit of ±34°.

For out-of-plane trajectories it is possible to improve the lighting conditions by rotating the S-IVB about the antenna axis. The improvement is in many cases limited by a constraint on the Saturn V stable platform middle gimbal angle and is not great enough to universally satisfy the withdrawal lighting conditions. The region of lunar landing longitudes for which withdrawal lighting is not satisfied is in this case reduced to sites east of 7° east longitude.

Spring withdrawal of the LM and ejection of SLA panels are under consideration. These modifications, if made, will relax the withdrawal constraints, and may permit all constraints to be satisfied.

L. P. Gieseler

2013-LPG-srb L. P. Gieseler

Attachments
- References
- Table I
- Figures 1 through 13
- Appendices I through IV

REFERENCES

1. "Joint MSFC/MSC AS-504 and Subsequent Missions Reference Constraints", Trajectory Document No. 67-FMP-3, March 15, 1967.

2. Boeing Co. Document No. D5-15481-1,"Saturn V AS-504 Launch Vehicle Reference Trajectory", Vol. II of II, Book 3, p. 10-71 to p. 10-149.

3. L. P. Gieseler, "The Influence of Earth Launch and Lunar Lighting Constraints on the Apollo Mission", Bellcomm Technical Memorandum TM-67-2013-4, May 26, 1967.

4. Ames and Murnaghan,"Theoretical Mechanics", Dover Publications, Inc., New York, 1957, p. 78.

5. Goldstein,"Classical Mechanics", Addison-Wesley Publishing Company Inc., 1959.

TABLE I - LUNAR ASCENDING NODES FOR 1969

Jan.	22
Feb.	19
March	18
April	14
May	12
June	8
July	5
Aug.	1
Aug.	29
Sept.	25
Oct.	23
Nov.	19
Dec.	16

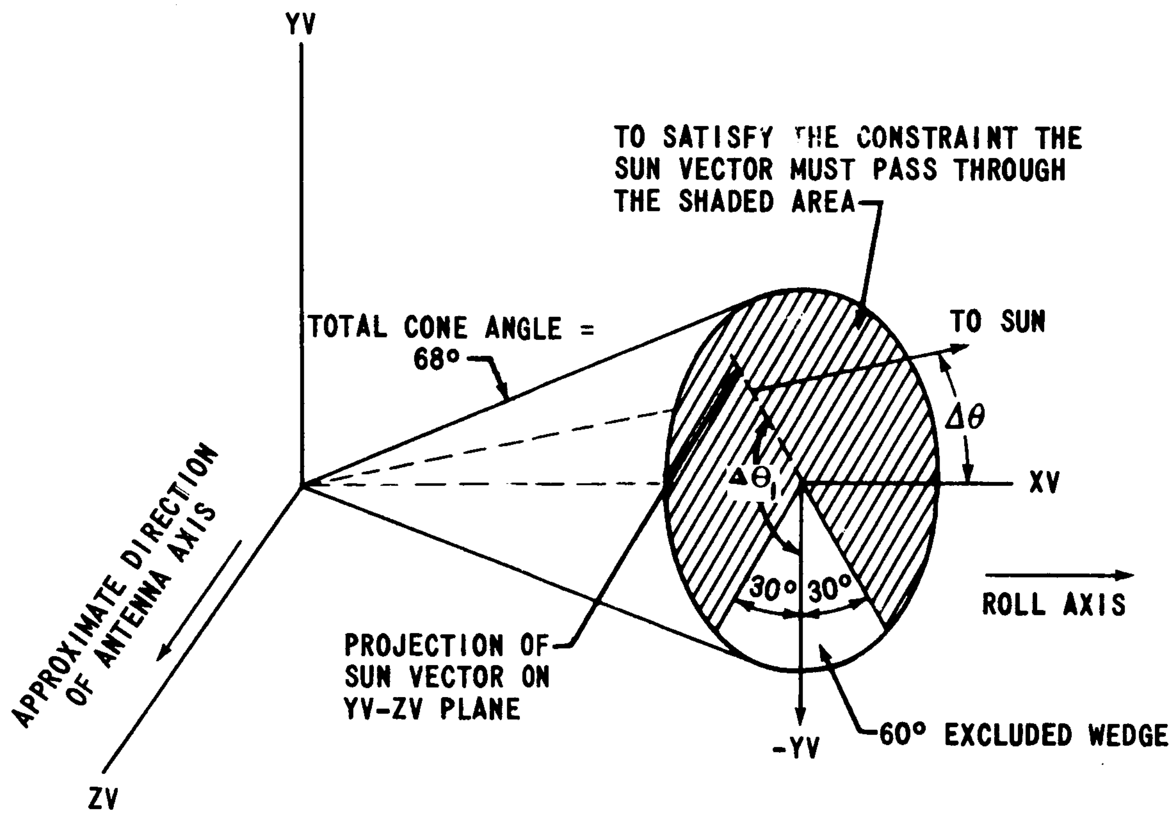

$|\Delta\theta| \leq 34°$

$|\Delta\theta_1| \geq 30°$

FIGURE I - S-IVB/SLA LIGHTING CONSTRAINT DURING WITHDRAWAL

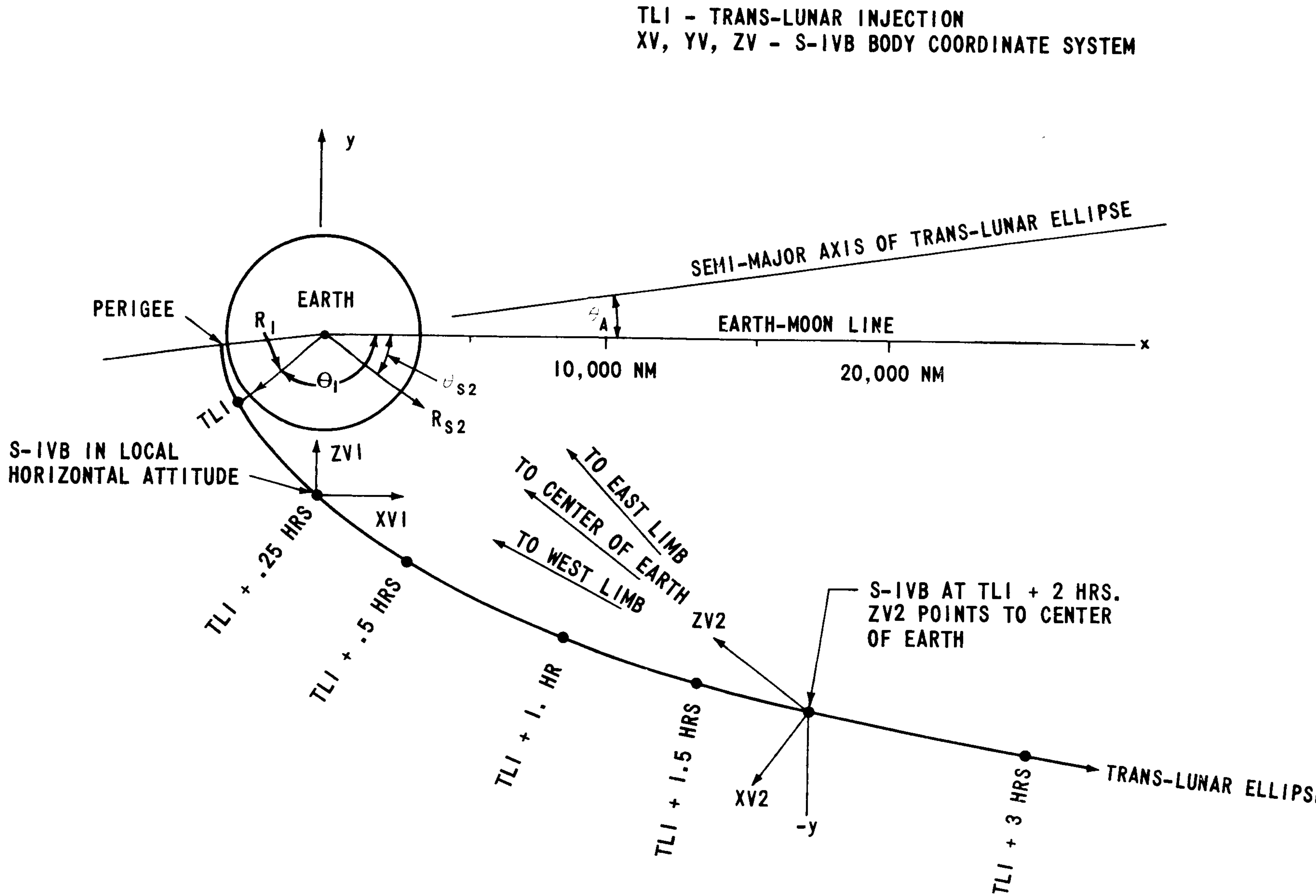

FIGURE 2 - FIRST THREE HOURS OF TRANS-LUNAR TRAJECTORY

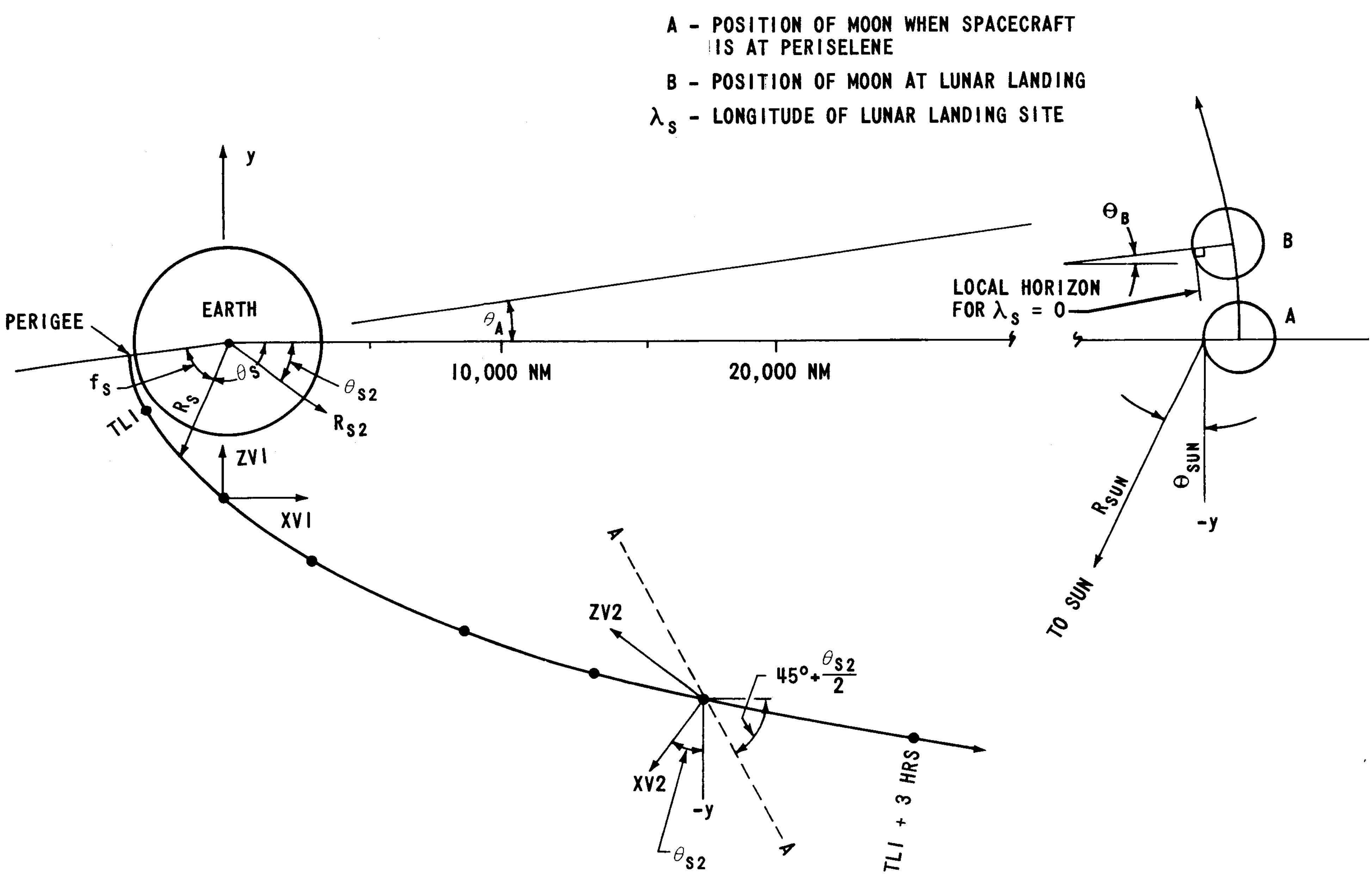

FIGURE 3 - GEOMETRY OF EARTH-MOON SYSTEM

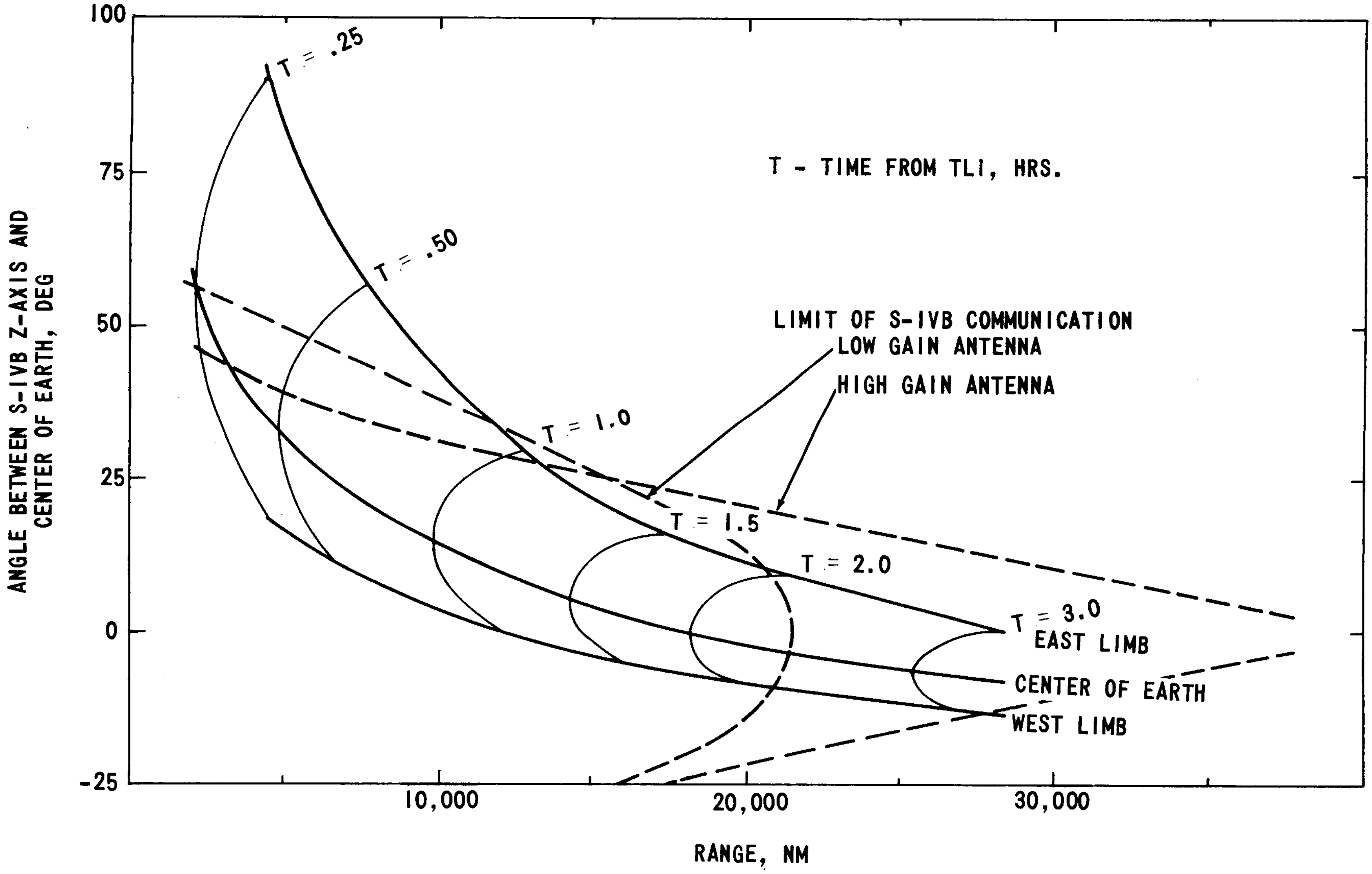

FIGURE 4 - ANGLES FROM S-IVB Z-AXIS

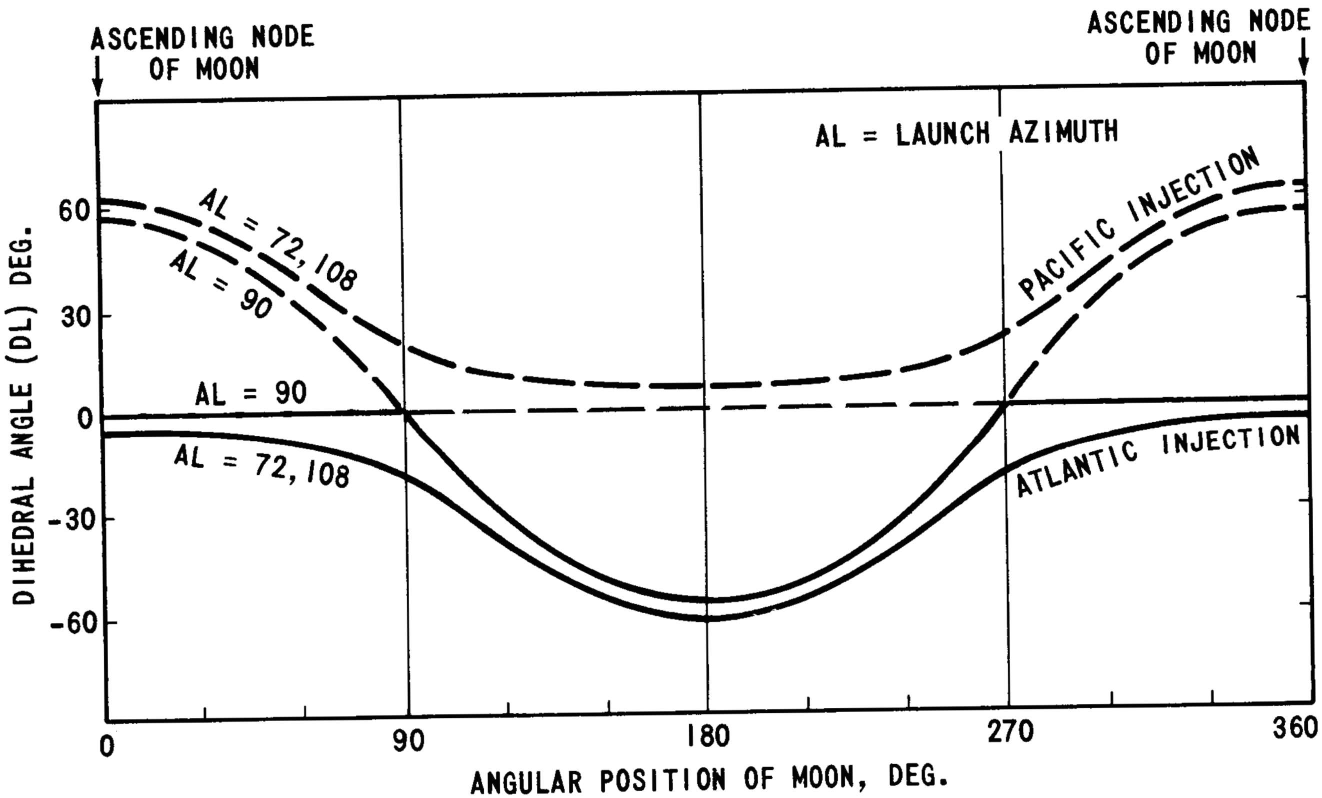

FIGURE 5 - BEHAVIOR OF THE DIHEDRAL ANGLES (DL) (1969)

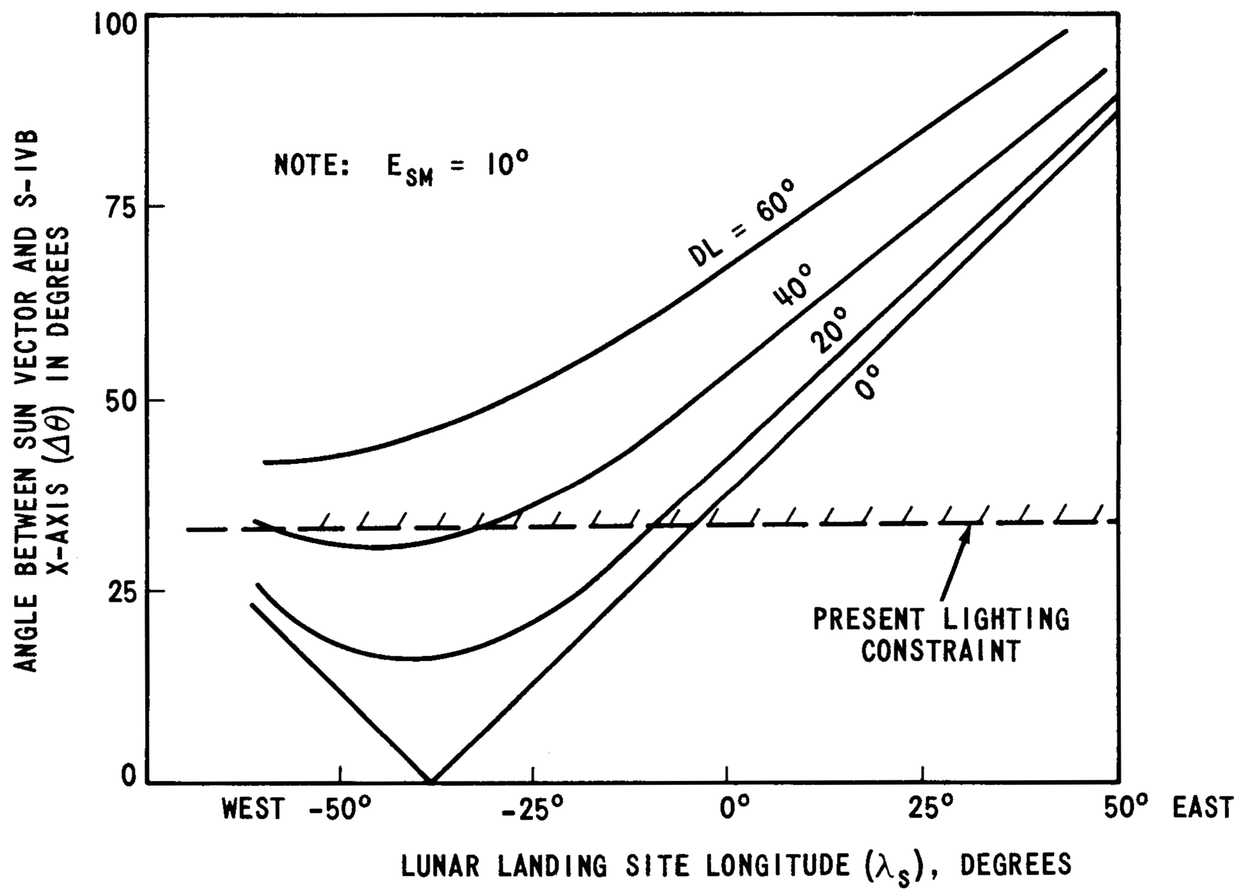

FIGURE 6 - LIGHTING DURING TRANSPOSITION AND DOCKING (REFERENCE ORIENTATION)

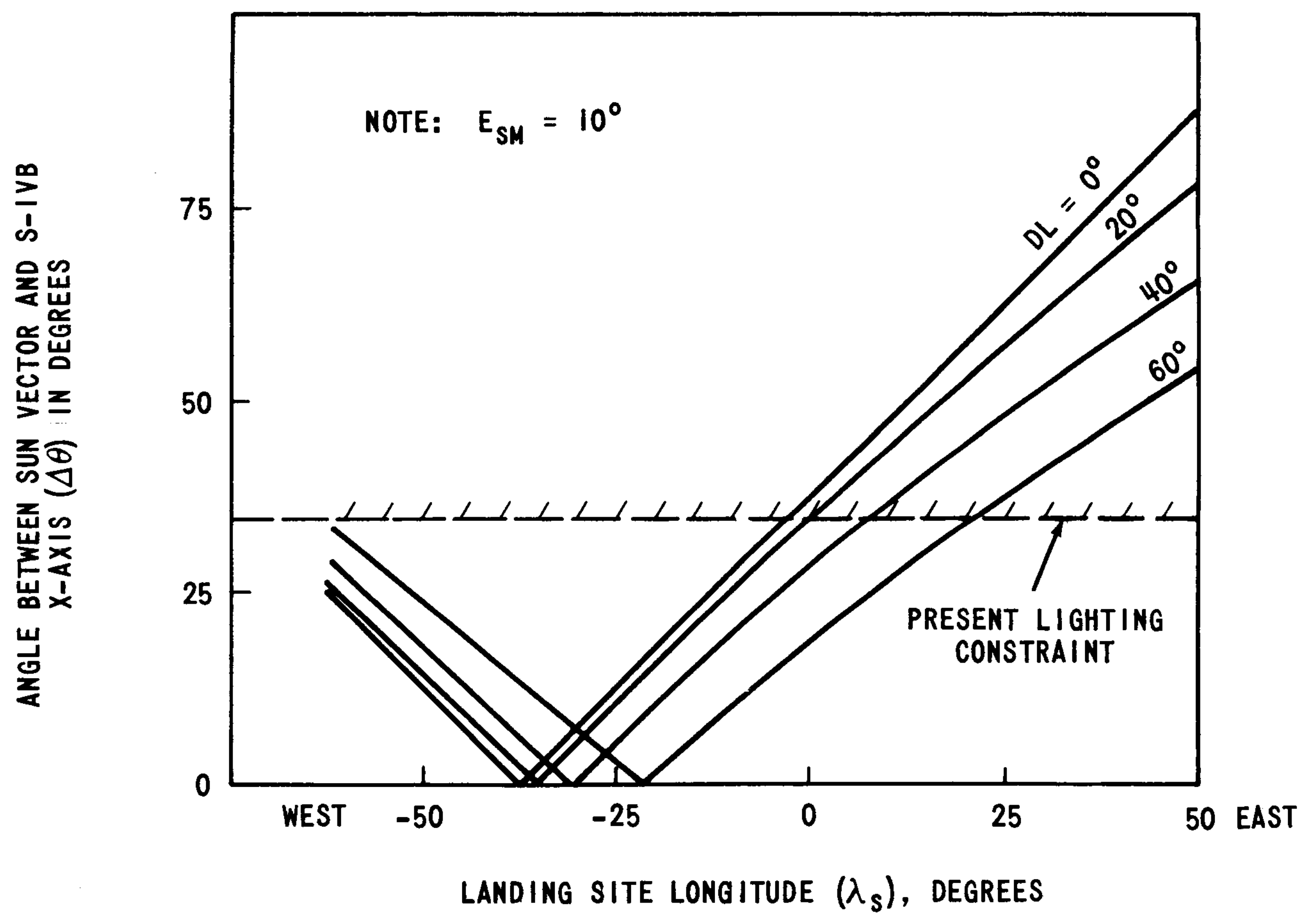

FIGURE 7 - LIGHTING DURING TRANSPOSITION AND DOCKING ($\Delta\theta$ MINIMIZED)

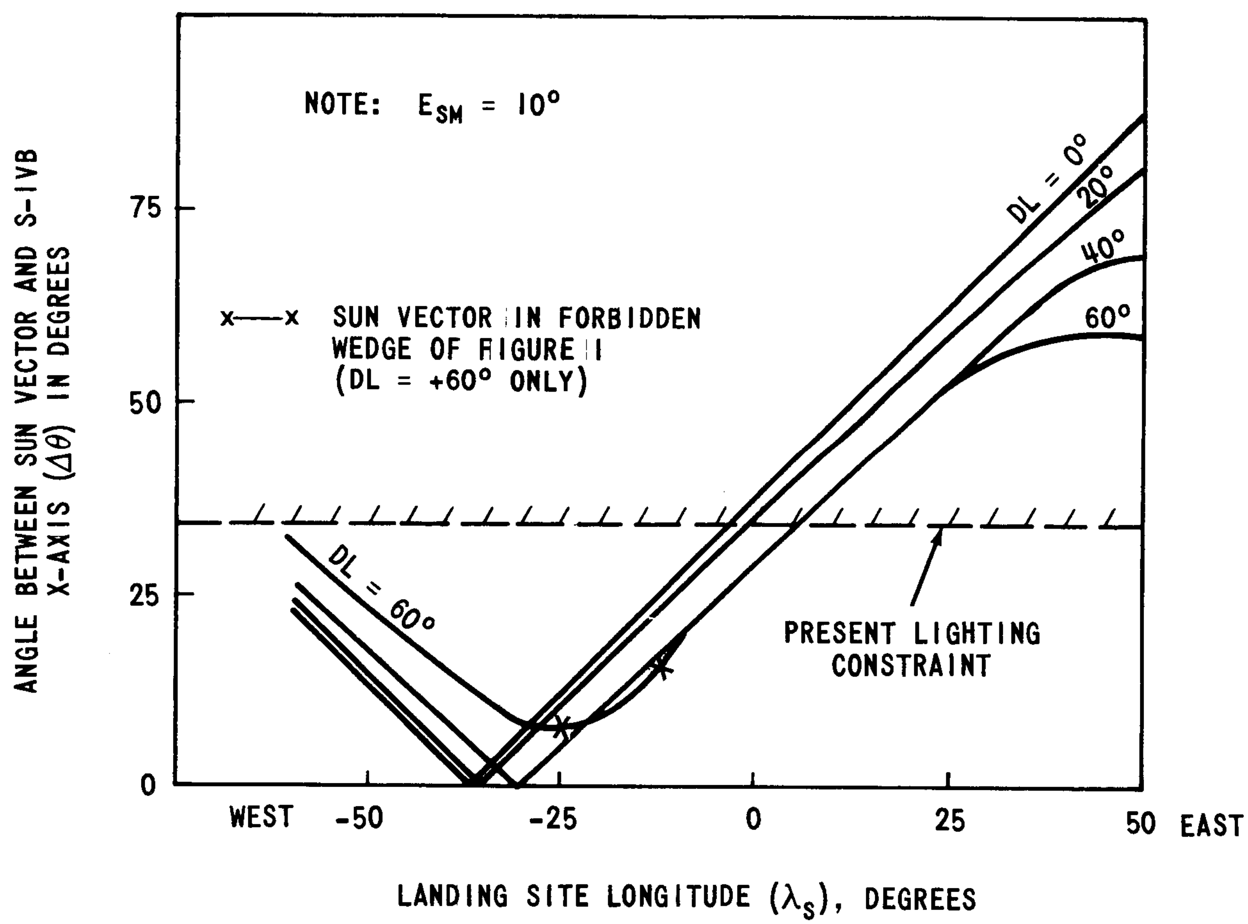

FIGURE 8 - LIGHTING DURING TRANSPOSITION AND DOCKING ($|\theta_m|$ CONSTRAINED TO $\leq 45°$)

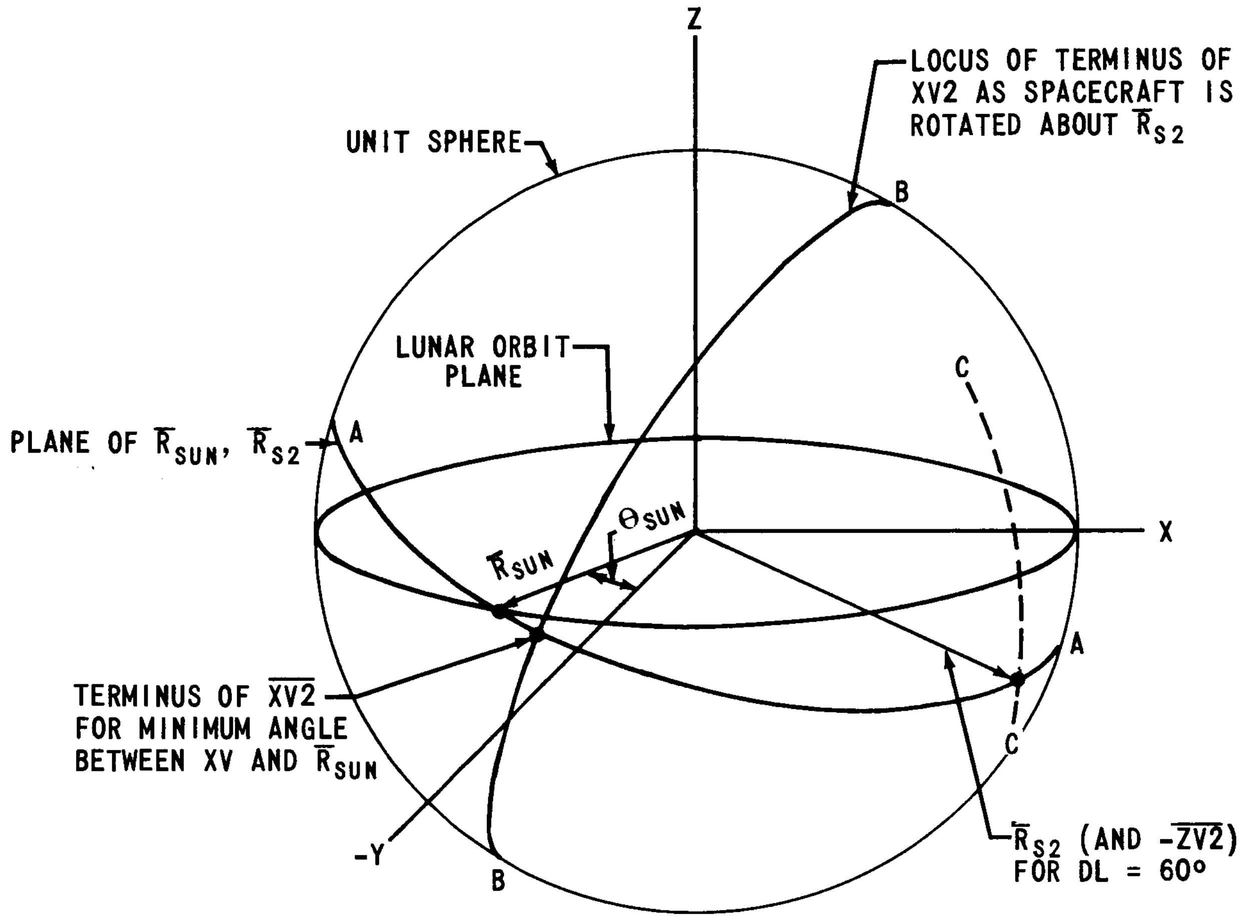

FIGURE 9 - COMPUTATION OF $\overline{XV2}$ FOR MINIMUM $|\Delta\Theta|$

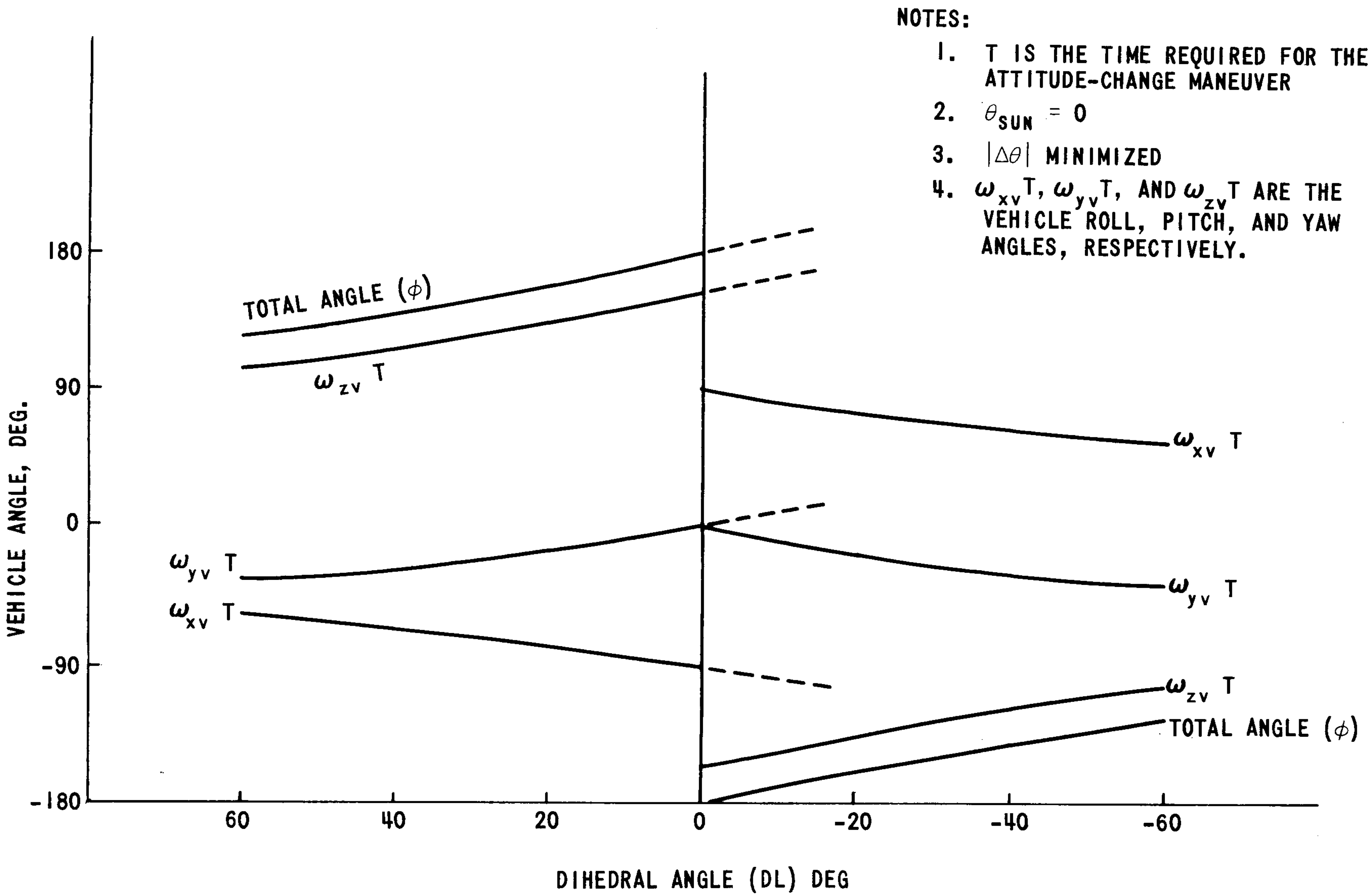

FIGURE 10 - SIMULTANEOUS ROTATIONS IN ROLL, PITCH, AND YAW

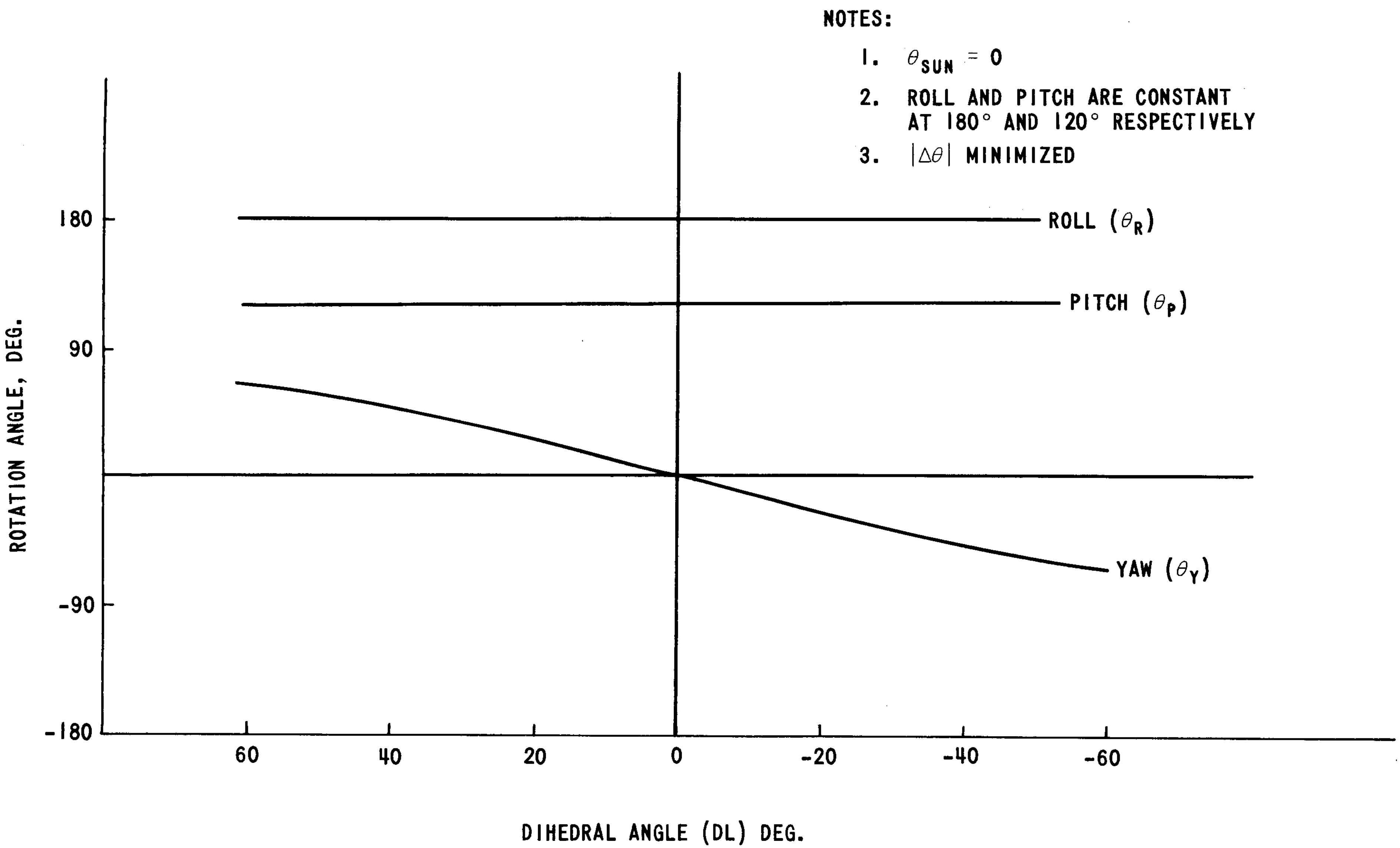

FIGURE 11 - SUCCESSIVE ROTATIONS IN PITCH, YAW, AND ROLL

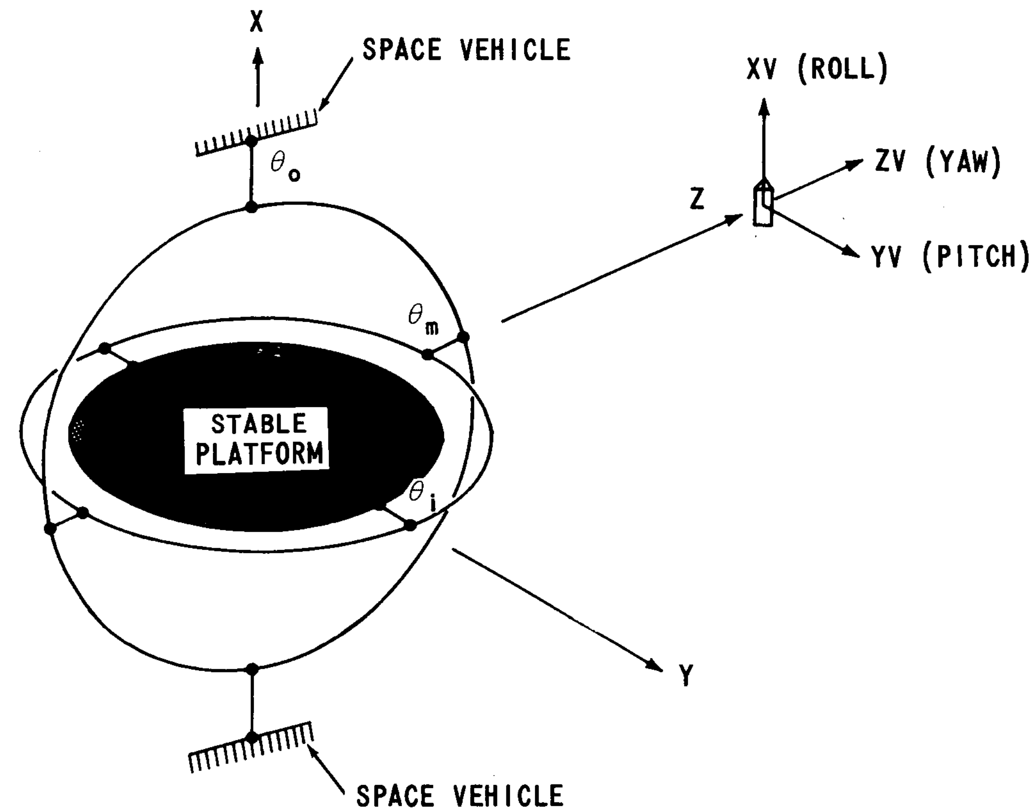

FIGURE 12 - GIMBAL ANGLES

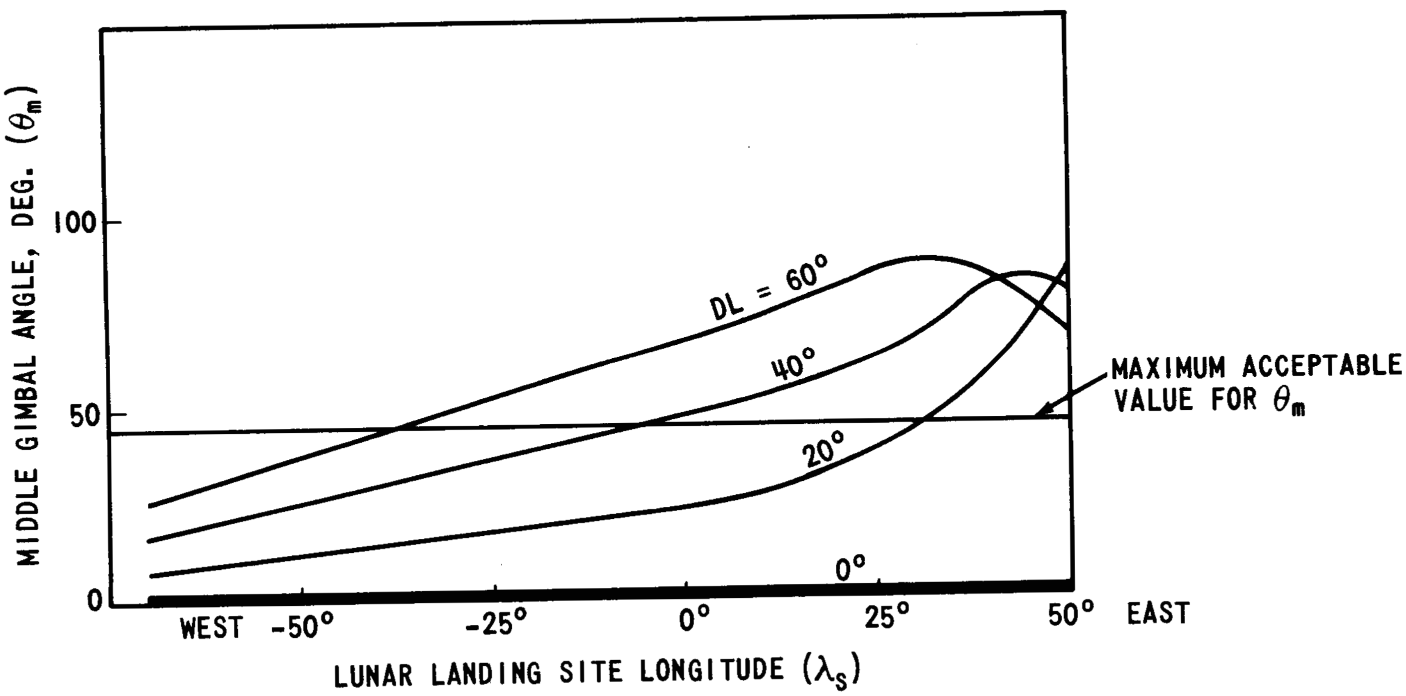

FIGURE 13 - MIDDLE GIMBAL ANGLE ($|\Delta\theta|$ OPTIMIZED)

APPENDIX I

List of Symbols

DL	Dihedral angle between translunar trajectory and lunar orbital planes measured positive for trajectories above the lunar orbit plane.
E_{sm}	Elevation of the sun above the eastern horizon at the lunar landing site.
f_S	True anomaly of a point on the ellipse.
$\overline{R}_1$	Radius vector of vehicle at TLI.
$\overline{R}_S$	Unit vector from the center of the earth to a point on the ellipse.
$\overline{R}_{S2}$	Same as $\overline{R}_S$ except that the point on the ellipse is the one located 2 hours from TLI.
$\overline{R}_{sun}$	Unit vector pointing to the sun.
V	Inertial velocity of vehicle at TLI, f.p.s.
x, y, z	Basic inertial coordinate system.
$\overline{XV}$, $\overline{YV}$, $\overline{ZV}$	Unit orthogonal coordinate system fixed in the vehicle.
$\overline{XV1}$, $\overline{YV1}$, $\overline{ZV1}$	$\overline{XV}$, $\overline{YV}$, $\overline{ZV}$ for the local horizon attitude between TLI and TLI + .25 hours.
$\overline{XV2}$, $\overline{YV2}$, $\overline{ZV2}$	$\overline{XV}$, $\overline{YV}$, $\overline{ZV}$ for the vehicle attitude during the transposition and docking period.
ϕ	Amount of rotation about axis of rotation, deg.
θ_1	Angle between the TLI point and the moon when the spacecraft is at periselene.
θ_A	Angle between semi-major axis and x axis.
θ_i, θ_m, θ_o	Inner, middle, and outer gimbal angles, respectively, of the Saturn stable platform.

θ_P, θ_Y, θ_R	Finite rotations about pitch, yaw and roll axes, respectively.
$\Delta\theta$	Angle between $\overline{R}_{sun}$ and $\overline{XV2}$ axis.
$\Delta\theta_1$	Angle between the projection of $\overline{R}_{sun}$ on the YV-ZV plane and the -YV axis.
θ_{sun}	Angle between $\overline{R}_{sun}$ and the -y axis.
θ_S	Angle between $\overline{R}_s$ and the x axis.
θ_{S2}	Angle between $\overline{R}_{S2}$ and the x axis.
β	Flight path angle at TLI.
λ_S	Lunar longitude of landing site.

Note: A matrix is identified by brackets [].

APPENDIX II

COMPUTATION OF VEHICLE ATTITUDE

This appendix describes the method used in this study for calculating the direction of the vehicle roll axis ($\overline{XV2}$) and the critical illumination angles $\Delta\theta$ and $\Delta\theta_1$. The ZV axis is assumed to be directed opposite to the radius vector at TLI + 2 hours.

A. Computation of $\overline{XV2}$ for the Reference Orientation (Figure 6).

Referring to Figure 3, θ_{S2} can be computed from Kepler's equation and Equation (2). For the in-plane case (DL=0), the direction cosines of $\overline{XV2}$ are:

$$
\begin{aligned}
XV2_x &= -\sin\,\theta_{S2} \\
XV2_y &= -\cos\,\theta_{S2} \qquad (6) \\
XV2_z &= 0
\end{aligned}
$$

For DL $\neq$ 0, $\overline{XV2}$ must be rotated about the x axis by the angle DL. The required formula is:

$$
\begin{aligned}
\overline{XV2}' = {} & \overline{x}(\overline{XV2} \cdot \overline{x})\,(1 - \cos\,DL) + \overline{XV2}\,\cos\,DL \\
& + (\overline{XV2} \times \overline{x})\,\sin\,DL \qquad (7)
\end{aligned}
$$

where $\overline{XV2}'$ is the rotated vector and $\overline{x}$ is the vector (1, 0, 0). Equation (7) is discussed in Reference (4).

B. Computation of $\overline{XV2}$ for Minimum $|\Delta\theta|$ (Figure 7).

Figure 9 is a pictorial view of vectors $\overline{R}_{sun}$, $\overline{XV2}$ and $\overline{R}_{S2}$, assuming that they have all been translated to the center of a unit sphere. The basic coordinate system is the same as that of Figures 2 and 3. The intersection of the plane defined by $\overline{R}_{sun}$ and $\overline{R}_{S2}$ with the surface of the sphere is shown in the figure as arc A-A.

It is known that $\overline{XV2}$ must be perpendicular to $\overline{R}_{S2}$ (since $-\overline{ZV}$ is colinear with $\overline{R}_{S2}$). When the vehicle is rotated about $\overline{R}_{S2}$ as an axis, $\overline{XV2}$ sweeps out a second plane B-B which is perpendicular to the first. It is evident from Figure 9 that the minimum angle between $\overline{XV2}$ and $\overline{R}_{sun}$ will be obtained when $\overline{XV2}$ lies in plane A-A. $\overline{R}_{sun} \times \overline{R}_{S2}$ is a vector perpendicular to the plane of $\overline{R}_{sun}$ and $\overline{R}_{S2}$, and $\overline{R}_{S2} \times (\overline{R}_{sun} \times \overline{R}_{S2})$ is a vector in the plane of $\overline{R}_{sun}$ and $\overline{R}_{S2}$, and normal to $\overline{R}_{S2}$. Then

$$\overline{XV2} = \frac{\overline{R}_{S2} \times (\overline{R}_{sun} \times R_{S2})}{|R_{S2} \times (R_{sun} \times R_{S2})|} \tag{8}$$

In Figure 9, planes A-A and B-B are the XV-ZV and XV-YV planes, respectively, for the orientation above. The YV-ZV plane is perpendicular to these two planes, and is indicated by C-C in the figure. The projection of $\overline{R}_{sun}$ on the YV-ZV plane can be seen to lie along vector $\overline{R}_{S2}$ which makes a 90° angle with $\overline{YV2}$. $\Delta\theta_1$ then always equals 90°, regardless of the value of θ_{S2} and DL, when the Saturn yaw constraint is not considered.

C. Computation of $\overline{XV2}$ and $\Delta\theta_1$ with $|\theta_m|$ Constrained to $<$ 45° (Figure 8).

It is shown in Appendix IV that $\theta_m = \sin^{-1}(\overline{YV1} \cdot \overline{XV2})$. When $|\theta_m| > 45°$ for the attitude computed in B above, a new attitude should be computed for which $|\theta_m| = 45°$. This is mathematically done by rotating $\overline{YV1}$ about $\overline{R}_{S2}$ through 45°, using Equation (7). The resulting vector is set equal to $\overline{XV2}$.

The direction of rotation is important, and in calculating the data of Figure 8, both directions were used. The selected attitude was the one with the smallest $\Delta\theta$.

To calculate $\Delta\theta_1$, it is necessary to determine the projections of the sun vector on the $\overline{ZV}$ and $-\overline{YV}$ axes of Figure 1. These are equal to $\overline{R}_{sun} \cdot \overline{ZV2}$ and $\overline{R}_{sun} \cdot -\overline{YV2}$ respectively. Then $\Delta\theta_1 = \tan^{-1} [(\overline{R}_{sun} \cdot \overline{ZV2})/(\overline{R}_{sun} \cdot -\overline{YV2})]$.

APPENDIX III

FORMULAS FOR COMPUTING ATTITUDE MANEUVERS

The problem to be solved in this Appendix can be expressed mathematically as follows: Given a vehicle-fixed coordinate system in an initial attitude defined by the three orthogonal unit vectors XV1, YV1, and ZV1, and the same coordinate system in a final attitude XV2, YV2, and ZV2. (These quantities are all vectors having 3 components in the basic x, y, z coordinate system of Figure 3. For simplicity the bar over the vectors will be omitted.) It is required to find the single rotation which will transform the initial attitude to the final one. Both the direction cosines of the axis of rotation and the magnitude of the angle of rotation are required. It is also required to find three successive rotations about the vehicle axes which will effect the same transformation. The pitch, yaw, roll maneuver will be used. However the technique described is general enough to apply to any other possible maneuver.

The basic equations are (Reference 3, pp. 95):

$$\begin{aligned} XV2 &= (XV2 \cdot XV1)XV1 + (XV2 \cdot YV1)YV1 + (XV2 \cdot ZV1)ZV1 \\ YV2 &= (YV2 \cdot XV1)XV1 + (YV2 \cdot YV1)YV1 + (YV2 \cdot ZV1)ZV1 \\ ZV2 &= (ZV2 \cdot XV1)XV1 + (ZV2 \cdot YV1)YV1 + (ZV2 \cdot ZV1)ZV1 \end{aligned} \tag{9}$$

The transformation matrix [TM] is given by:

$$[TM] = \begin{bmatrix} a_{11} & a_{12} & a_{13} \\ a_{21} & a_{22} & a_{23} \\ a_{31} & a_{32} & a_{33} \end{bmatrix} \tag{10}$$

where

$$\begin{aligned} a_{11} &= XV2 \cdot XV1; \; a_{12} = XV2 \cdot YV1; \; a_{13} = XV2 \cdot ZV1 \\ a_{21} &= YV2 \cdot XV1; \; a_{22} = YV2 \cdot YV1; \; a_{23} = YV2 \cdot ZV1 \\ a_{31} &= ZV2 \cdot XV1; \; a_{32} = ZV2 \cdot YV1; \; a_{33} = ZV2 \cdot ZV1 \end{aligned} \tag{11}$$

Equation (9) is then equivalent to the matrix equation:

$$\begin{bmatrix} XV2 \\ YV2 \\ ZV2 \end{bmatrix} = [TM] \begin{bmatrix} XV1 \\ YV1 \\ ZV1 \end{bmatrix} \tag{12}$$

Let B be the vector axis of rotation with components B_{xv}, B_{yv}, B_{zv} in the vehicle coordinate system and components B_x, B_y, B_z in the basic coordinate system. From Reference 3, pp 119,

$$\begin{aligned} (a_{11}-1)B_{xv} + a_{12}B_{yv} + a_{13}\, B_{zv} &= 0 \\ a_{21}B_{xv} + (a_{22}-1)B_{yv} + a_{23}\, B_{zv} &= 0 \\ a_{31}B_{xv} + a_{32}B_{yv} + (a_{33}-1)B_{zv} &= 0 \end{aligned} \tag{13}$$

It is known that the determinant made up of coefficients of Equation 13 equals zero, and that a solution can be obtained by using any two of the equations to solve for two of the unknowns in terms of the third. For example:

$$B_{xv} = \frac{a_{12}a_{23} - a_{13}(a_{22}-1)}{(a_{11}-1)\ (a_{22}-1) - a_{12}a_{21}}\, B_{zv}$$

$$B_{yv} = \frac{a_{13}a_{21} - a_{23}\ (a_{11}-1)}{(a_{11}-1\ (a_{22}-1) - a_{12}a_{21}}\, B_{zv}$$

Now let $B_{zv} = 1$, and $r = \sqrt{B_{xv}2 + B_{yv}2 + 1}$. Then if b is a unit vector corresponding to B, $b_{xv} = B_{xv}/r$, $b_{yv} = B_{yv}/r$, and $b_{zv} = 1/r$. These direction cosines are referred to either of the two sets of vehicle axes. The direction cosines referred to the basic coordinate system are given by:

$$
\begin{aligned}
bl_x &= b_{xv}\, XVl_x + b_{yv}\, YVl_x + b_{zv}\, ZVl_x \\
bl_y &= b_{xv}\, XVl_y + b_{yv}\, YVl_y + b_{zv}\, ZVl_y \\
bl_z &= b_{xv}\, XVl_z + b_{yv}\, YVl_z + b_{zv}\, ZVl_z
\end{aligned}
\tag{15}
$$

The above equations are similar to one of the equations (9) with the components written out in detail. The single rotation angle ϕ which corresponds to the above axis of rotation is given by (Reference 3, pp.123-124):

$$
\cos\phi = \frac{1}{2}\,(a_{11} + a_{22} + a_{33} - 1) \tag{16}
$$

The angular velocity ω about the axis of rotation is equal to ϕ/T, where T is the time required to perform the attitude change maneuver. Since ω is a vector quantity (as opposed to sequential rotations), it can be resolved into its components ω_{xv}, ω_{yv} and ω_{zv}. These are the vehicle roll, pitch, and yaw rates respectively, applied simultaneously. Then

$$
\begin{aligned}
\omega_{xv} &= \frac{\phi}{T} \times b_{xv} \\
\omega_{yv} &= \frac{\phi}{T} \times b_{yv} \\
\omega_{zv} &= \frac{\phi}{T} \times b_{zv}
\end{aligned}
\tag{17}
$$

The variation of the above quantities as DL is changed from $-60°$ to $+60°$ is shown in Figure 10 for $\theta_{sun} = 0$. Note that the total angle is greatest at DL = 0, where it equals either $+180°$ or $-180°$. These two quantities are mathematically equivalent since $\omega T = 360° - \omega T$. However physically they correspond to rotation rates having opposite directions. The discontinuities shown can be avoided by confining the curve for the total angle to positive values only. The dotted curves will then result. However the angle through which the vehicle must be rotated is greater than before, and this maneuver would not normally be as desirable.

The transformation matrices for sequential rotations about the vehicle axes are: (Reference 3, pp. 109)

$$[ROLL] = \begin{bmatrix} 1 & 0 & 0 \\ 0 & \cos\theta_R & \sin\theta_R \\ 0 & -\sin\theta_R & \cos\theta_R \end{bmatrix}$$

$$[PITCH] = \begin{bmatrix} \cos\theta_P & 0 & -\sin\theta_P \\ 0 & 1 & 0 \\ \sin\theta_P & 0 & \cos\theta_P \end{bmatrix} \qquad (18)$$

$$[YAW] = \begin{bmatrix} \cos\theta_Y & \sin\theta_Y & 0 \\ -\sin\theta_Y & \cos\theta_Y & 0 \\ 0 & 0 & 1 \end{bmatrix}$$

The transformation matrix for the pitch, yaw, roll maneuver is given by

$$[TM] = [roll]\ [yaw]\ [pitch] \qquad (19)$$

Upon multiplying out the matrices we obtain

$$a_{11} = \cos\theta_Y \cos\theta_P \qquad (20a)$$

$$a_{12} = \sin\theta_Y \qquad (20b)$$

$$a_{13} = -\cos\theta_Y \sin\theta_P \qquad (20c)$$

$$a_{22} = \cos\theta_R \cos\theta_Y \qquad (20d)$$

$$a_{32} = -\sin\theta_R \cos\theta_Y \qquad (20e)$$

From (20b)

$$\theta_Y = \sin^{-1} a_{12} \qquad (21)$$

It is known that θ_Y is restricted to the first and fourth quadrants. Then cos θ_Y is positive, and from (20a) and (20c)

$$\theta_P = \tan^{-1} \frac{-a_{13}}{a_{11}} \qquad -180° \leq \theta_P \leq +180° \qquad (22)$$

Also from (20d) and (20e)

$$\theta_R = \tan^{-1} \frac{-a_{32}}{a_{22}} \qquad -180° \leq \theta_R \leq +180° \qquad (23)$$

The variation of the above quantities as DL is changed from -60° to +60° is shown in Figure 11 for $\theta_{sun} = 0°$. When DL = 0, $\theta_Y = 0$, and the maneuver degenerates into the pitch, roll maneuver described in Section 7.0. For DL = ±60°, $\theta_Y = \mp 65°$, as shown. Figure 11 indicates that θ_R is constant at 180°. From equation (23), a_{32} must equal zero and from equation (11), this means that ZV2 must be perpendicular to YV1 regardless of the value of DL. A study of Figure 3 will show that this is indeed the case. In addition it can be seen that $\theta_R = 180°$ regardless of the value of θ_{sun}.

Figure 11 also indicates that θ_P is constant at 120°. From equation (22) this means that a_{13}/a_{11} is independent of DL. However this relationship is too complex to visualize directly from Figure 3.

The above method of determining θ_P, θ_Y and θ_R can be applied to any maneuver made up of sequential rotations about orthogonal vehicle-fixed axes. It is only necessary to change equation (19) to conform to the desired maneuver sequence, and then to perform the required matrix multiplications using equation (18). The rotation angles can then be calculated from five of the nine elements. It is not necessary that the maneuver use all three vehicle axes. In fact the classical Euler angles as described in Reference (3) pp. 107 correspond to the equation

$$[TM] = [yaw]\,[roll]\,[yaw] \tag{24}$$

Upon multiplying out the matrices using equation (18) it is found that

$$\theta = \cos^{-1} a_{33}$$

$$\phi = \tan^{-1} \frac{a_{31}}{-a_{32}}$$

$$\psi = \tan^{-1} \frac{a_{13}}{a_{23}}$$

where θ is the roll angle, ϕ the first yaw angle, and ψ the second. These are also the Euler angles.

APPENDIX IV

GIMBAL ANGLES

The stable platform of the guidance system is connected to the space vehicle as shown in Figure 12. The inner, middle, and outer gimbal angles are shown there as θ_i, θ_m, and θ_o respectively. These angles are assumed to be referenced to a zero position which is left unspecified. The magnitude of these angles as computed below then represents a gimbal angle change resulting from a maneuver from one attitude to another. Figure 12 also shows the orientation of the vehicle-fixed coordinate system at launch, indicating that θ_i is associated with pitch, θ_m with yaw, and θ_o with roll. This relationship however may be changed by subsequent vehicle maneuvers, except for θ_o, which is always associated with roll.

The stable platform remains in a fixed attitude in inertial space. Gimbal lock occurs when θ_m assumes a value which brings the θ_i axis coincident with the θ_o axis. Thus θ_m must be restricted to a range of values centered about the value for which the θ_o and θ_i axis are perpendicular. θ_i and θ_m however can take on any value without affecting the orientation of the gimbal axes relative to each other. In addition θ_i can be varied freely without changing the gimbal axes relative to the vehicle axes. This means that when starting from the configuration of Figure 12 the vehicle can be pitched by any amount without changing the relative orientation of the various coordinate axes shown there. The theoretical development given in Appendix III requires that the three axes of rotation be mutually perpendicular at all times. For this reason the attitude maneuvers described there cannot use the gimbal axes as axes of rotation.

It was indicated in Section 7.0 that the same final attitude can be achieved by a number of different maneuvers. However the construction of the gimbals gives a particular importance to successive rotations in pitch, yaw, and roll. When starting from the configuration of Figure 12 this maneuver will result in changes in θ_i, θ_m, and θ_o which are respectively equal to the pitch, yaw, and roll rotations. During the pitch rotation only θ_i will change, during the yaw rotation only θ_m will change, and during the roll rotation only θ_o will change. Equations (21), (22), and (23) of Appendix III then also apply to the gimbal angles, even if the pitch, yaw, roll sequence is not the one that is actually used. The equation for θ_m is especially simple:

$$\theta_m = \sin^{-1} a_{12} = \sin^{-1} (YV1 \cdot XV2) \qquad (24)$$

This equation was used to compute θ_m for the same values of DL and λ_S plotted in Figure 7. The results are shown in Figure 13. A maximum acceptable value of 45° for θ_m is also indicated in the figure. It can be seen that positive values of λ_S and large values of DL tend to give unacceptably large values of θ_m. This assumes that prior to the attitude maneuver the inner and outer gimbal axes are perpendicular.